N78-32464

IMPETUS OF COMPOSITE MECHANICS ON TEST METHODS FOR FIBER COMPOSITES

C. C. CHAMIS

LEWIS RESEARCH CENTER
CLEVELAND, OHIO

1978

DISCLAIMER NOTICE

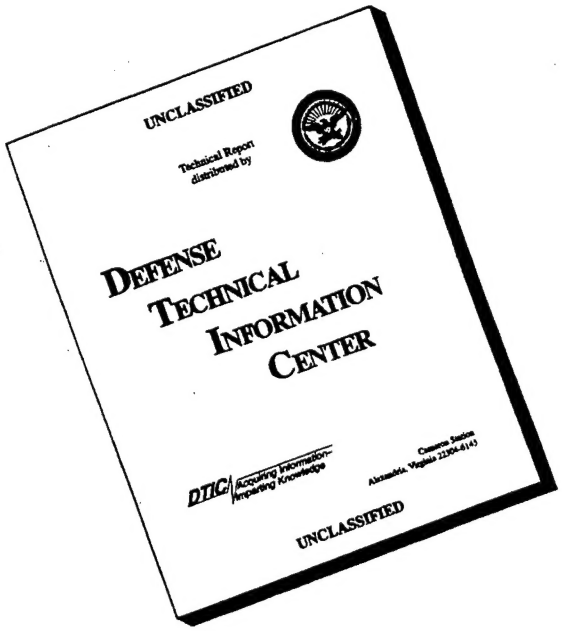

THIS DOCUMENT IS BEST QUALITY AVAILABLE. THE COPY FURNISHED TO DTIC CONTAINED A SIGNIFICANT NUMBER OF PAGES WHICH DO NOT REPRODUCE LEGIBLY.

NASA Technical Memorandum 78979

IMPETUS OF COMPOSITE MECHANICS ON TEST METHODS FOR FIBER COMPOSITES

C. C. Chamis
Lewis Research Center
Cleveland, Ohio

TECHNICAL PAPER to be presented at the
US-USSR Seminar on "Fracture of Composite Materials"
Riga, USSR, September 4-7, 1978

1. Report No.	2. Government Accession No.	3. Recipient's Catalog No.
NASA TM-78979		

4. Title and Subtitle	5. Report Date
IMPETUS OF COMPOSITE MECHANICS ON TEST METHODS FOR FIBER COMPOSITES	6. Performing Organization Code

7. Author(s)	8. Performing Organization Report No.
C. C. Chamis	E-9734
	10. Work Unit No.

9. Performing Organization Name and Address	11. Contract or Grant No.
National Aeronautics and Space Administration Lewis Research Center Cleveland, Ohio 44135	
	13. Type of Report and Period Covered
12. Sponsoring Agency Name and Address	Technical Memorandum
National Aeronautics and Space Administration Washington, D.C. 20546	14. Sponsoring Agency Code

15. Supplementary Notes

16. Abstract

The impetus of composite mechanics on the composite test methods and/or on interpreting test results is described using examples from the three major areas of composite mechanics: composite micromechanics, composite macromechanics and laminate theory. The specific examples described occurred over the last 12-years and include contributions such as criteria for selecting resin matrices for improved composite strength, the 10° off-axis tensile test, criteria for configuring hybrids and superhybrids for improved impact resistance and the "reduced bending rigidities" concept for buckling and vibration analyses.

17. Key Words (Suggested by Author(s))	18. Distribution Statement
Composite mechanics; Micromechanics; Macromechanics; Laminate theory; Buckling; Reduced bending stiffness; Strength, impact; Residual stresses; Quasi-isotropic analogy; Superhybrids; 10° Off-axis; Tests	Unclassified - unlimited STAR Category 39

19. Security Classif. (of this report)	20. Security Classif. (of this page)	21. No. of Pages	22. Price*
Unclassified	Unclassified		

* For sale by the National Technical Information Service, Springfield, Virginia 22161

IMPETUS OF COMPOSITE MECHANICS ON TEST METHODS FOR FIBER COMPOSITES

by C. C. Chamis

National Aeronautics and Space Administration
Lewis Research Center
Cleveland, Ohio 44135

INTRODUCTION

Over the last twelve years composite mechanics has contributed significantly to the development of test methods for composites, to the interpretation of test results and, thereby, to the immense progress of the whole composites technology. In this paper, significant contribution of the three major areas of composite mechanics (composite micromechanics, composite macromechanics and laminate theory) to the development of test methods are illustrated with selected examples. The selected examples are limited to those with which the author was personally involved. However, these examples cover contributions over a time span of about ten years and can be considered as being representative of the contribution of composite mechanics to the development of composite test methods.

The specific examples describe contributions such as criteria for selecting resin matrices for improved composite strength, the 10^{o} off-axis tensile test, procedures for configuring hybrids and the concept of "reduced bending rigidities." The pertinent composite mechanics equations associated with each contribution are given and are supplemented by tabular and/or graphical data which illustrate the significance of the contribution. The symbols are defined when they are first used and are summarized in the appendix for convenience.

COMPOSITE MICROMECHANICS

The impetus of composite micromechanics in identifying constituent properties which influence composite strength is illustrated herein using two examples: (1) matrix properties influencing composite transverse tensile, compressive and intralaminar shear strengths (ref. 1) and major constituent contributors to composite impact resistance (ref. 2).

Matrix Properties Influencing Composite Transverse Tensile, Compressive and Intralaminar Shear Strengths

Stress-strain curves for high and low modulus matrix resins are shown in figures 1(a) and (b), respectively. Also included in the figures is the stress-strain curve for a unidirectional composite tested in the transverse direction. It can be seen from figure 1 that only the initial portion of the matrix stress/strain curve is utilized in the composite. The notation to be used in subsequent discussion is defined in figure 1. Note that the matrix limit strain, ϵ_{mpT}, is taken to be the point at which the matrix stress/strain curve exhibits a pronounced nonlinearity.

The governing micromechanics equations are from reference 1:

Transverse tensile strength ($S_{\ell 22T}$)

$$S_{\ell 22T} = \beta_{22T} \frac{\epsilon_{mpT}}{\beta_v \varphi_{\mu 22}} E_{\ell 22} \tag{1}$$

Transverse compressive strength ($S_{\ell 22C}$)

$$S_{\ell 22C} = \beta_{22C} \frac{\epsilon_{mpC}}{\beta_v \varphi_{\mu 22}} E_{\ell 22} \tag{2}$$

Intralaminar shear strength ($S_{\ell 12S}$)

$$S_{\ell 12S} = \beta_{12} \frac{\epsilon_{mpS}}{\beta_v \varphi_{\mu 12}} G_{\ell 12} \tag{3}$$

The undefined notation in equations (1), (2), and (3) is as follows: β denotes the theory experiment correlation coefficient reflecting the fabrication process; β_v denotes the void influence; φ_μ is the matrix-strain-magnification factor; the subscripts T, C, and S denote tension, compression, and shear, respectively; ϵ_{mpT} is the matrix limit strain as defined from figure 1; and correspondingly for compression and shear; $E_{\ell 22}$ and $G_{\ell 12}$ are the composite transverse and shear moduli, respectively.

There are three groups of variables with distinct physical meaning in equations (1), (2), and (3). These groups can be easily identified by writing equation (1) in the following form:

$$S_{\ell 22T} = \left(\frac{\beta_{22T}}{\beta_v}\right)\left(\frac{E_{\ell 22}}{\varphi_{\mu 22}}\right)\epsilon_{mpT} \tag{1a}$$

where (β_{22T}/β_v) represents the particular fabrication process and depends only on the fabrication process; $(E_{\ell 22}/\varphi_{\mu 22})$ is defined herein as the "strength parameter" which depends on the local and average composite geometry and on the elastic properties of the constituents; and ϵ_{mpT} is the matrix limiting strain as defined previously. Corresponding variables in equations (2) and (3) can be grouped in the same fashion with analogous physical interpretations.

The matrix variables influencing $S_{\ell 22T}$ enter through either $(E_{\ell 22}/\varphi_{\mu 22})$ or ϵ_{mpT}. The group (β_{22T}/β_v) does not depend (at least not explicitly) on the matrix elastic or strength properties.

The variation of $(E_{\ell 22}/\varphi_{\mu 22})$ and $(G_{\ell 12}/\varphi_{\mu 12})$ with matrix modulus for a Thornel-50/epoxy composite with a 0.5 fiber volume fraction and zero voids is shown in figures 2 and 3, respectively. As can be seen in figures 2 and 3 the matrix modulus markedly affects the transverse and shear strength parameters.

The results in figures 2 and 3 suggest that transverse and intralaminar shear strength tests should be sensitive to matrix modulus.

The variation of the transverse strength parameter ($E_{\ell 22}/\varphi_{\mu 22}$) with fiber volume ratio is shown in figure 4 for three matrix moduli, zero voids and 10 percent voids. The curves in figure 4 show that the transverse strength parameter is sensitive to both matrix modulus and void content. However, it is not as sensitive to fiber volume ratio. These observations also apply to the intralaminar shear strength parameter.

The above composite micromechanics results guided the experimental investigation described in reference 1. The combined results led to a simple criterion for selecting resin matrices for improved composite strength. This criterion as stated in reference 1 is: "Of the various simple matrix properties, the area under the matrix stress/strain curve up to the proportional limit strain (initial area) is the best index for assessing matrix influence on composite strength and overall composite structural behavior." An even simpler version of this criterion is: "The initial modulus of the resin stress-strain curve is a good index in assessing the contribution of the resin matrix to composite strength." The higher the initial modulus the higher the composite strength. It is interesting to note that the total elongation-to-fracture of the resin does not influence composite strength (ref. 1).

Major Constituent Contributors to Composite Impact Resistance

The total energy stored in a uniformly stressed unidirection composite under uniaxial tension along the fiber direction is simply

$$U = \frac{1}{2}\epsilon^{*}_{\ell 11T} S_{\ell 11T} V \tag{4}$$

or

$$U = \left(\frac{S^{2}_{\ell 11T}}{2E_{\ell 11}}\right) V \tag{5}$$

where U is the strain energy, ϵ^* is the fracture strain, S is the fracture strength, V is the volume, and E is the modulus. The subscript group $\ell 11T$ is defined as follows: ℓ refers to unidirectional properties, 11 identify outward normal to the plane and stress directions in that order, and T identifies the sense of the stress. Using composite micromechanics $S_\ell 11T$ and E_{211} are expressed in terms of fiber and matrix properties (ref. 2). The impact energy density (IED) equals the strain energy divided by the volume. The IED of composites with an E_f/E_m ratio greater than 20 is approximated by

$$\text{IED} = \frac{(1 - k_v)k_f\beta_{fT}^2 S_{fT}^2}{2E_f} \tag{6}$$

with an approximation error of less than 5 percent. The variables in equation (6) are as follows: k_v and k_f denote void and fiber volume ratios, respectively; β_{fT} represents the in-situ fiber strength efficiency which reflects the fabrication process. The subscript f refers to fiber property. The important points to be noted in equation (6) are the quadratic dependence of the strain energy density on the fiber strength S_{fT}^2 and the fabrication process variable β_{fT}^2. For a high impact resistance composite, equation (6) imposes the following requirements: a high strength low modulus fiber, approximately 100 percent fiber properties translation efficiency, high fiber volume ratio, and low void volume ratio.

The transverse IED is given by

$$\text{IED} = \frac{1}{2}\left(\beta_{22}\frac{\epsilon_{mPT}}{\beta_v \varphi_{\mu 22}}\right)^2 E_{\ell 22} \tag{7}$$

where the notation has been defined in equations (1) to (3). As was the case for equation (1), the important resin property for transverse IED is the modulus (E_m).

The ranking of IED of various composites predicted using equations (6) and (7) are compared with measured data in table I. As can be seen the comparison is excellent.

COMPOSITE MACROMECHANICS

The impetus of composite macromechanics in developing test methods for characterizing unidirectional composites is illustrated herein using the 10^{o} off-axis test method (ref. 3). A schematic of the test specimen for this method is shown in figure 5.

The composite macromechanics equations used in developing the 10^{o} off-axis test method for intralaminar shear characterization are respectively (refer to fig. 6): plain stress transformation

$$\begin{Bmatrix} \epsilon_{\ell 11} \\ \epsilon_{\ell 22} \\ \epsilon_{\ell 12} \end{Bmatrix} = \begin{bmatrix} \cos^2\theta & \sin^2\theta & \frac{1}{2}\sin 2\theta \\ \sin^2\theta & \cos^2\theta & -\frac{1}{2}\sin 2\theta \\ -\sin 2\theta & \sin 2\theta & \cos 2\theta \end{bmatrix} \begin{Bmatrix} \epsilon_{cxx} \\ \epsilon_{cyy} \\ \epsilon_{cxy} \end{Bmatrix} \tag{6}$$

or in matrix form

$$\{\epsilon_{\ell}\} = [R_{\ell}]\,\{\epsilon_{c}\} \tag{6a}$$

plain stress transformation for uniaxial loading (fig. 6)

$$\sigma_{\ell 11} = \sigma_{cxx}\cos^2\theta;\ \sigma_{\ell 22} = \sigma_{cxx}\sin^2\theta;\ \sigma_{\ell 12} = \frac{1}{2}\sigma_{cxx}\sin 2\theta \tag{7}$$

and the two dimensional failure criterion

$$1 - \left[\left(\frac{\sigma_{\ell 11}}{S_{\ell 11T}}\right)^2 + \left(\frac{\sigma_{\ell 22}}{S_{\ell 22T}}\right)^2 - K_{\ell 12}\left(\frac{\sigma_{\ell 11}}{S_{\ell 11T}}\right)\left(\frac{\sigma_{\ell 22}}{S_{\ell 22T}}\right) + \left(\frac{\sigma_{\ell 12}}{S_{\ell 12S}}\right)\right] \geq 0 \tag{8}$$

The undefined notation in equations (6) to (8) is as follows: ϵ denotes strain; σ denotes stress; θ is the angle between load or composite axis and mate-

rial axis (along fiber) (fig. 6); S denotes strength and $K_{\ell 12}$ is a function of the elastic properties of the composite (ref. 4). The subscript ℓ denotes material axis property and c denotes composite axis property. The subscript T and S denote tension and shear, respectively.

The variation of the material-axes strains as a function of load angle is plotted in figure 7 for a Mod-I/epoxy unidirectional composite. As can be observed in this figure, the material-axes shear strain (intralaminar shear strain $\epsilon_{\ell 12}$) is maximum at about a 10° load orientation angle and appears to be insensitive to small errors about this angle. These are significant results that led to the recommendation of the 10° off-axis tensile test specimen to measure the intralaminar shear modulus and fracture shear stress. Other composites, for example, approach their peaks at about 11° for T-300/epoxy (PR288) and 15° for S-glass/epoxy (PR288).

The fracture stress of a 10° off-axis specimen (ref. 3) is 343 MPa (49.8 ksi) which is equal to σ_{cxx} in equation (7). The material axes stresses from equation (7) are, respectively: $\sigma_{\ell 11}$ = 333 MPa (48.3 ksi); $\sigma_{\ell 22}$ = 10 MPa (1.5 ksi); and $\sigma_{\ell 12}$ = 59 MPa (8.5 ksi). The strengths are: $S_{\ell 11T}$ = 563 MPa (81.7 ksi); $S_{\ell 22T}$ = 28 MPa (4 ksi) and $S_{\ell 12S}$ = 52 MPa (7.6 ksi). The parameter $K_{\ell 12}$ = 1.44 from reference 3. Using these numerical values in equation (8) yields:

$$1 - \left[\left(\frac{48.3}{81.7}\right)^2 + \left(\frac{1.5}{4.0}\right)^2 - 1.44\,\frac{48.3 \times 1.5}{81.7 \times 4.0} + \left(\frac{8.5}{7.6}\right)^2\right]$$

which reduces to

$$1 - [0.350 + 0.141 - 0.319 + 1.25] = -0.421$$

Since this value is less than zero, according to the failure criterion, fracture has occurred. The important observation to be noted here is that the major stress contribution to fracture is from the intralaminar shear stress which is the last term in the brackets. The contribution from the longitudinal and

transverse stresses (first three terms in the brackets) tend to cancel each other. It is worth noting that the cancellation tendency observed here is not exhibited when the relative magnitudes are compared on an individual stress basis. The numerical results from the combined-stress failure criterion just discussed lead to the conclusion that fracture of the 10° off-axis tensile specimen is initiated by the intralaminar shear stress.

Therefore, the use of composite macromechanics helped identify the two important features, peak shear strain and shear stress, that induced fracture at the 10° plane. These features led to the recommendation of the 10° off-axis tensile test method for intralaminar shear characterization. Comparisons of intralaminar shear modulus and strength as measured using the 10° off-axis tensile test with literature data are shown in table II (ref. 3). As can be seen the data from the 10° off-axis tensile specimen are within the range of the literature data.

LAMINATE THEORY

Several examples are described in this section in order to illustrate the impetus of linear laminate theory (LLT) or testing composites and on interpreting composite behavior. These examples include configuring hybrid composite laminates, lamination residual stresses, laminate warpage, and the quasi-isotropic laminate analogy for planar randomly reinforced fiber composites.

Criteria for Configuring Hybrid Composite Laminates

The influence of the constituent plies on the section properties and thermal forces of hybrid composite laminates is best illustrated by briefly examining the general LLT equations for determining these properties:

$$[A],[C],[D] = \sum_{i=1}^{N_\ell} \left[\int_{Z_{i-1}}^{Z_i} (1, Z, Z^2)\, [R]^T [E]^{-1} [R]\, dz \right]_i \tag{9}$$

$$\{N_T\}, \{M_T\} = \sum_{i=1}^{N_\ell} \left[\int_{Z_{i-1}}^{Z_i} (1, Z)\, \Delta T\, [R]T [E]^{-1} \{\alpha\}\, dZ \right]_i \tag{10}$$

The notation in equations (9) and (10) is as follows: [A], [C], and [D] denote membrane, coupling and flexural (bending) stiffness matrices, respectively; these matrices are $[3 \times 3]$ for plane problems and $[5 \times 5]$ in cases where the transverse (through the thickness) shear deformations are taken into account. The term Z denotes the laminate thickness coordinate referred to some convenient plane; the index i denotes the i^{th} ply in the stacking sequence of the laminate; $[R]_i$ denotes the transformation matrix locating the i^{th} ply material axes (parallel to and transverse to the fiber direction) from the laminate structural axes (coincident with the principal load direction (eq. (6a)); $[E]_i$ denotes the i^{th} ply strain-stress relations; $\{N_T\}$ and $\{M_T\}$ denote the thermal forces and moments; ΔT_i denotes the difference between ply and reference temperature; and $\{\alpha\}_i$ denotes the ply thermal expansion coefficients.

Referring to equation (9), it is seen that the constituent plies influence the hybrid section properties (1) through the ply-strain stress relations $[E]_i$, (2) the ply orientation relative to the hybrid structural axes $[R]_i$, and (3) the ply location in the stacking sequence Z_i. Laminate configuration concepts such as the core/shell hybrid and the super-hybrid are readily deduced from equation (9). The ply properties used in equation (9) for interply hybrids are obtained either by measurement or by the use of micromechanics. The ply properties for intraply hybrids are presently obtained by measurement.

The force deformation relationships for a composite laminate are given by

$$\left\{\begin{array}{c}\{N_c\}\\ \hline \{M_c\}\end{array}\right\} = \left[\begin{array}{c|c}[A] & [C]\\ \hline [C] & [D]\end{array}\right] \left\{\begin{array}{c}\{\epsilon_{co}\}\\ \hline \{\kappa_c\}\end{array}\right\} + \left\{\begin{array}{c}\{N_T\}\\ \hline \{M_T\}\end{array}\right\} \tag{11}$$

The undefined notation in equation (11) is as follows: $\{N_c\}$ denotes force, or stress resultant at the section, $\{M_c\}$ is the corresponding moment, $\{\epsilon_{co}\}$ denotes the reference plane strains, $\{\kappa_c\}$ denotes the coresponding curvature and $\{N_T\}$ and $\{M_T\}$ the thermal forces and moments, respectively.

The LLT equation that has been used to predict ply strains in laminates and in hybrid composite laminates may be expressed in matrix form as follows:

$$\{\epsilon\}_i = [R]_i [A]^{-1} \langle \{N_c\} + \{N_T\} + [C] \{\kappa_c\} \rangle - Z_i [R]_i \{\kappa_c\} \tag{12}$$

where $\{\epsilon\}_i$ denotes the strains in the i^{th} ply. The other symbols have been defined previously. Note that the thermal moments are included in $\{\kappa_c\}$.

The equation to predict ply stress is obtained by multiplying equation (12) with the ply stress-strain relations and accounting for the free thermal strains. The resulting matrix equation may be expressed as follows:

$$\{\sigma\}_i = [E]_i^{-1} \langle \{\epsilon\}_i - \Delta T_i \{\alpha\}_i \rangle \tag{13}$$

where $\{\sigma\}_i$ denotes the stresses in the i^{th} ply of the hybrid, $\{\epsilon\}_i$ is determined from equation (12), and the other symbols have been defined previously.

Equations (9) to (13) were used to configure the superhybrid composites shown in figure 8 (ref. 5). Briefly, the concept of superhybrid composites involves the strategic location of the titanium foil and B/Al plies to provide maximum resistance to transverse and shear forces. A direct way to assess whether this is achieved in superhybrids is to compute the ply stress influence coefficients due to uniaxial membrane and bending composite stresses. These influence coefficients are computed using the LLT equations (9) to (13).

Selected results obtained for a superhybrid are summarized in table III. These results are for a particular ply type as it is first encountered progressing inward from the surface. Note that to obtain the ply stress, the influence coefficients must be multiplied by the membrane (bending) stress taken with the correct sign.

As can be observed from the data in table III, the titanium foil and B/Al plies have large ply stress influence coefficients for uniaxial transverse and shear composite stresses. Therefore, the titanium foils and the B/Al in the superhybrids provide practically all the resistance for transverse and shear forces. This verifies their role in the superhybrid concept. Note in table III that the ply stress influence coefficients of the adhesive are negligible for all uniaxial composite stresses. Therefore, fracture will occur first in one of the nonadhesive constituents as desired in the superhybrid concept.

Laminates Residual Stresses

The LLT equation for predicting lamination residual stresses in angleplied laminates is given in (ref. 6)

$$\{\sigma\}_i = [E]_i^{-1} \langle [R]_i \{\epsilon_{co}\} - Z_i [R]_i \{\kappa_c\} - \Delta T_i \{\alpha\}_i \rangle \qquad (14)$$

where $\{\epsilon_{co}\}$ and $\{\kappa_c\}$ are obtained from equation (11) with $\{N_c\} = \{M_c\} = 0$. Equation (14) in conjunction with composite micromechanics can be used to predict the effects of laminate configuration, fiber volume ratio and void volume ratio on the ply residual stresses. Ply residual transverse stress for two angleplied laminates from high-modulus/polyimide-matrix composite system versus fiber volume ratio are plotted in figure 9. Corresponding results versus void volume ratio are plotted in figure 10. The plots in figure 9 show that the transverse ply stresses are relatively high compared to corresponding strength and will, therefore, cause the type of transply cracks shown in figure 11. Also, the laminate configuration and the fiber volume

ratio have a strong effect on the ply residual stress while the void volume ratio has negligible effect.

These results were confirmed by the experimental data of references 7 and 8. The results were also used to recommend laminate configurations for jet engine compressor fan blades to avoid transply cracks (ref. 9).

Laminate Warpage Due to Thermal Stress

Unsymmetric angleplied laminates will warp when subjected to changes in temperature. Unsymmetries caused by ply misorientation produce warpage in flat laminates upon removal from the mold (ref. 10). A schematic of a warped laminate is depicted in figure 12. The corner deflection (at point C, fig. 12) is given by

$$w(x, y) = \frac{1}{2} \kappa_{yy} b^2 + \kappa_{xy} ab \tag{15}$$

where the curvatures are determined from LLT equation (11) with $N_c = M_c = 0$. The required equation is

$$\begin{Bmatrix} \{\epsilon_{co}\} \\ \hline \{\kappa_c\} \end{Bmatrix} = \begin{bmatrix} [A] & [C] \\ \hline [C] & [D] \end{bmatrix}^{-1} \begin{Bmatrix} \{N_T\} \\ \hline \{M_T\} \end{Bmatrix} \tag{16}$$

where $\{\kappa_c\}^T = [\kappa_{xx}, \kappa_{yy}, \kappa_{xy}]$, [A], [C], and [D] are given by equation (9) and $\{N_T\}$ and $\{M_T\}$ are given by the LLT equation (10). Equations (15), (16), (10) and (9) can used to determine the possible degree of ply misorientation in angleplied laminates which warp due to temperature changes.

This procedure was used to determine the possible ply misorientation in two warped laminates: $[0_2/\pm 30]_S$ and $[0_2 \pm 45]_S$ (ref. 10). These laminates were 30.5 cm (12 in.) square plates and were made from Modmor I/ epoxy (ref. 10). These laminates warped when they were cooled from cure temperature (about 461 K (370° F)) to room temperature (294 K (70° F)). The corner desplacements measured at point C, figure 12, were 0.56 cm

(0.22 in.) for the $[0_2/\pm30]_S$ angleplied laminate and 3.05 cm (1.2 in.) for the $[0_2/\pm45]_S$ angleplied laminate. Note that these warpage corner deflections are relatively large when compared to the laminate thickness of 0.15 cm (0.06 in.). Possible ply misorientations which will yield comparable corner deflections using equations (9), (10), (16), and (15), were as follows: $[0_2/30.4/-30/-30/30/0_2]$ and $[0_2/\pm45/\mp39/0_2]$. As can be seen, the perturbations were 0.4° for the $[0_2/\pm30]_S$ laminate and 6.0° for the $[0_2/\pm45]_S$. These perturbations are relatively small and can be caused inadvertently during the fabrication process. A large number of other possible combinations of ply misorientations exist which will produce comparable corner deflections.

The important point from the above discussion is that LLT can be used effectively to identify problems resulting from the fabrication process.

Quasi-Isotropic Analogy

Linear laminate theory (LLT) can be used to determine the influence of ply misorientation on the modulus and Poisson's ratio (elastic properties) of quasi-isotropic (π/n) laminates. The elastic properties are determined from the array [A], equation (9). The results can then be used to assess the elastic behavior of planar randomly reinforced composites (PRRC) because of the elastic properties equivalence that exists between quasi-isotropic laminates and PRRC (ref. 11).

The influence of 5° ply misorientations in the 0° plies of π/n (n = 3, 4, 6, and 8) quasi-isotropic laminates on composite modulus is shown in figure 13 and for Poisson's ratio in figure 14 (ref. 12). In these figures the modulus and Poisson's ratio are plotted versus load angle (between load and 0° ply directions) for all four laminates. As can be seen both modulus and Poisson's ratio approach their respective "No Misorientation" straight line as n becomes progressively larger.

The important conclusion from the plots in figures 13 and 14 is that PRRC would require at least 8 different fiber directions at any section through the laminate thickness to achieve isotropic elastic behavior.

Reduced Bending Rigidities for Buckling and Vibration Analysis of Laminates with Coupled Responses

The buckling and vibration analysis of composite laminates having coupled responses such as bending-stretching and/or twisting-stretching requires the solution of the nonlinear anisotropic plate equations. However, approximate buckling loads and vibration frequencies can be determined using the "reduced bending rigidities" method. The method is easily derivable from the LLT equation (11). The details are described in reference 13.

The governing equation for the reduced bending rigidities is given by

$$[D_R] = [D] - [C]^T [A]^{-1} [C] \tag{17}$$

where $[D_R]$ is the array of the "reduced bending rigidities." The other arrays were defined in equation (11). The values of these arrays are given in table IV for a specific laminate. The buckling load obtained using the "reduced bending rigidities" from table IV in the computational procedure described in reference 13 is 65.8 kN/m (376 lb/in). This value is in very good agreement with the measured value 65.0 kN/m (371 lb/in) and with that from nonlinear finite element analysis 69.0 kN/m (394 lb/in). The buckling load obtained using orthotropic plate buckling equations such as those in reference 14 is 154 kN/m (680 lb/in) which is 80-percent higher than the measured value. Vibration frequencies are treated in a similar fashion.

The important conclusion from the above discussion is that LLT was effectively used to obtain a good solution to a complex buckling problem and, therefore, was essential in interpreting properly the experimental results.

SUMMARY

The impetus of composite mechanics on test methods and on the proper interpretation of test results has been reviewed using selected examples. The examples include composite micromechanics, composite macromechanics, and laminate theory. The examples selected demonstrate the following:

1. Composite micromechanics was the essential ingredient required to identify simple tests for identifying resin matrix properties that contribute to improved composite strength and for identifying the major constituent contributors to impact resistance.

2. Composite macromechanics was necessary in the development of the 10° off-axis tensile test for intralaminar shear characterization. Three aspects of composite mechanics that were necessary are: strain transformation, stress transformation and combined-stress failure.

3. Laminate theory is essential for; configuring hybrids for improved impact resistance, for assessing lamination residual stress on laminate strength, for identifying possible or inadvertent ply misorientations, for interpreting what may be thought to be low buckling loads of composite plates which exhibit coupling and for identifying sensitive tests to experimentally measure the effects of all of these.

4. Composite mechanics, in general, has contributed significantly to the advancement of composite technology through its impetus on the development of discriminating test methods and through its extensive usage in interpreting test results.

APPENDIX - SYMBOLS

a	plate edge-x dimension
b	plate edge-y dimensions
deg	degree
E	modulus
G	shear modulus
IED	impact energy density
$K_{\ell 12}$	Coupling coefficient, combined stress failure criterion
k_f	fiber volume ratio
k_v	void ratio
LLT	linear laminate theory
N_ℓ	number of plies
n	number of ply angles to yield quasi-isotropic laminate
N_{LD}	number of delaminated layers
S_ℓ	unidirectional composite (ply) strength
S*	modified S, eq. (17) and (A56)
PRRC	planar randomly reinforced composites
S_{fT}	fiber strength
T	temperature
ΔT	temperature difference between composite processing and use temperatures
U	energy, strain energy
V	volume
w	plate lateral displacement (parallel to z-axis)
x, y, z	structural axes coordinate system

z_i	distance to the i^{th} ply from the reference plane
1,2,3	material axes coordinate system
α	thermal coefficient of expansion
β	correlation coefficients
β_v	void strain magnification on in-situ matrix
ϵ	strain
ϵ^*	composite limit fracture strain
ϵ_{mp}	matrix in situ limit strain, cap subscript denotes type
θ	ply angle measured from the structural x-axis to the material 1-axis
φ_μ	matrix strain-magnification-factor
σ	stress

Subscripts:

C	compression
c	composite
f	fiber property
i	summation index
L	longitudinal
ℓ	undirectional composite (ply) property
m	matrix property
mp	matrix limiting property
R	residual stress, reduced
S	shear
T	tension, temperature
x,y,z	directions coinciding with structural axes
1,2,3	directions coinciding with material axes

ARRAYS AND VECTORS

A	Array of composite axial stiffnesses referred to composite structural axes
C	Array of composite coupling stiffnesses referred to composite structural axes
D	Array of composite bending (flexural) stiffnesses referred to composite structural axes
D_R	Reduced bending rigidities
E	Array of strain-stress relations (elastic constants for the i^{th} ply)
M	Vector of moments or unbalanced thermal moments referred to composite structural axes
N	Vector of forces or unbalanced thermal forces referred to composite structural axes
R_ℓ	Array of transformation coefficients
α	Vector of thermal coefficients of expansion of the i^{th} ply
ϵ	Vector of strains
ϵ_{co}	Vector of composite strains referred to composite structural axes at the reference plane
κ_{cx}	Vector of composite local curvatures referred to composite structural axes

REFERENCES

1. Chamis, C. C.; Hanson, M. P.; and Serafini, T. T.: Criteria for Selecting Resin Matrices for Improved Composite Strength. Mod. Plast., vol. 50, no. 5, May 1973, pp. 90-106. (Also NASA TM X-68166, 1973.)

2. Chamis, Christos C.; Hanson, Morgan P.; and Serafini, Tito T.: Impact Resistance of Unidirectional Composites. Composite Materials: Testing and Design, ASTM Spec. Tech. Publ. 497, 1972, pp. 324-349. (Also NASA TN D-6463, 1971.)

3. Chamis, C. C.; and Sinclair, J. H.: Ten-degree Off-Axis Test for Shear Properties in Fiber Composites. Exp. Mech., vol. 17, no. 9, 1977, pp. 339-346. Also NASA TN D-8215, 1976.

4. Chamis, C. C.: Failure Criteria for Filamentary Composites. Composite Materials: Testing and Design, Am. Soc. Test. Mater. Spec. Tech. Publ. 460, 1969, pp. 336-351. Also NASA TN D-5367, 1969.

5. Chamis, C. C.; Lark, R. F.; and Sullivan, T. L.: Superhybrid Composites an Emerging Structural Material. NASA TM X-71836, 1975.

6. Chamis, C. C.: Lamination Residual Stresses in Cross-plied Fiber Composites. Proceedings of the 26th Annual Technical Conference of the Reinforced Plastics/Composite Institute, Society of the Plastics Industry, Inc., 1971, Section 17-D, pp. 1-12. Also NASA TM X-52881, 1970.

7. Daniel, I. M.; and Liber, T.: Measurement of Lamination Residual Strains in Graphite Fiber Laminates. Presented at Federation of Materials Societies. Second International Conference on Mechanical Behavior of Composite Materials, ICM-II, Boston, MA, Aug. 16-20, 1976.

8. Daniel, I. M.; and Liber, T.: Effects of Laminate Construction on Residual Properties of Composites. Soc. Exp. Stress Anal. 1976 Spring Meeting, Paper No. WR-45-1975.

9. Hanson, M. P.; and Chamis, C. C.: Experimental and Theoretical Investigation of HT-S/PMR-PI Composites for Application to Advanced Aircraft Engines. Proceedings of the 29th Annual Technical Conference of the Reinforced Plastics/Composite Institute, Society of the Plastics Industry, Inc., 1974, Section 16-C, pp. 1-10. Also NASA TN D-7698, 1974.

10. Chamis, C. C.: A Theory for Predicting Composite Laminate Warpage Resulting from Fabrication. Proceedings of the 30th Anniversary Technical Conference of the Reinforced Plastics/Composite Institute, Society of the Plastics Industry, Inc., 1975, Section 18-C, pp. 1-9. Also NASA TM X-71619, 1975.

11. Chamis, C. C.: Design Properties of Randomly Reinforced Fiber/Resin Composites. Proceedings of the 27th Annual Technical Conference of the Reinforced Plastics/Composites Institute, Society of the Plastics Industry, Inc., 1972, Section 9-D, pp. 1-10. Also NASA TM X-67948, 1972.

12. Sullivan, T. L.: Elastic Properties and Fracture Strength of Quasi-Isotropic Graphite/Epoxy Composites. NASA TM X-73592, 1977.

13. Chamis, C. C.: Buckling of Anisotropic Composite Plates. J. Struct. Div., Am. Soc. Civ. Eng., vol. 95, no. ST10, Proc. Paper 6799, Oct. 1969, pp. 2119-2139.

14. Lekhnitskii, S. G.: Anisotropic Plates. Second ed. Gordon and Breach, 1968.

TABLE I. - MINIATURE IZOD IMPACT DATA FOR FIBER/EPOXY COMPOSITES (Ref. 2)

Fiber	Type	Fiber volume ratio	Average impact energy				Rank			
			Longitudinal		Transverse		Longitudinal		Transverse	
			cm-N	in.-lb	cm-N	in.-lb	Measured	Predicted	Measured	Predicted
Graphite	Thornel-50S	0.532	85.9	7.6	7.9	0.7	5	5	3	3
	Thornel-50	.583	208.0	18.4	3.4	.3	4	4	5	5
	HTS	.523	56.5	5.0	14.7	1.3	6	6	2	2
	Modmor-I	.542	215.0	19.0	4.5	.4	3	3	4	4
Glass	S	0.486	757.0	67.0	15.8	1.4	1	1	1	1
Kev-49	----------	-----	280.0	24.8	3.4	0.3	2	2	5	---

TABLE II. - COMPARISON OF MEASURED INTRALAMINAR SHEAR PROPERTIES FROM 10^{o} OFF-AXIS TENSILE SPECIMEN WITH THOSE REPORTED ELSEWHERE (REF. 3)

Composite	10^{o} Off-axis tensile specimen		Reported elsewhere				10^{o} Off-axis tensile specimen		Reported elsewhere			
			Low		High				Low		High	
	Modulus						Fracture stress					
	N/cm^2	psi	N/cm^2	psi	N/cm^2	psi	N/cm^2	ksi	N/cm^2	ksi	N/cm^2	ksi
Mod-I/epoxy	0.61×10^6	0.88×10^6	0.44×10^6	0.64×10^6	0.62×10^6	0.90×10^6	5.9×10^3	8.6	4.7×10^3	6.8	6.1×10^3	8.9
T-300/epoxy	.43	.63	.42	.61	.69	1.00	8.3	12.1	6.2	9.0	9.2	13.3
S-glass/epoxy	.65	.94	.57	.83	1.2	1.74	7.1	10.3	4.5	6.5	12	17.1

TABLE III. - PREDICTED PLY STRESS INFLUENCE COEFFICIENTS DUE TO UNIT UNIAXIAL COMPOSITE STRESS FOR SUPER-HYBRID (Ti, B/Al, Gr/Ep), (REF. 5)

Ply	Uniaxial Membrane Stress					Uniaxial Flexural Stress[a]				
	Longitudinal		Transverse		Shear	Longitudinal		Transverse		Shear
	Longitudinal	Transverse	Longitudinal	Transverse		Longitudinal	Transverse	Longitudinal	Transverse	
Top										
Titanium alloy	0.824	0.032	0.373	1.95	2.08	0.768	0.026	0.161	1.22	1.28
Adhesive	0.011	0.002	0.009	0.028	0.024	0.010	0.002	0.004	0.016	0.014
B/Al	1.63	-0.014	0.184	2.45	2.43	1.12	-0.013	-0.017	1.13	1.10
Gr/Ep	0.912	-0.002	-0.184	0.226	0.206	0.420	0	-0.095	0.070	0.063
Center										
Gr/Ep	0.912	-0.002	-0.184	0.226	0.206	-0.420	0	0.095	-0.070	-0.063
B/Al	1.63	-0.014	0.184	2.45	2.43	-1.12	0.013	0.017	-1.13	-1.10
Adhesive	0.011	0.002	0.009	0.028	0.024	-0.010	-0.002	-0.004	-0.016	-0.014
Titanium alloy	0.824	0.032	0.373	1.95	2.08	-0.768	-0.026	-0.161	-1.22	-1.28
Bottom										

[a] To obtain ply stress, multiply influence coefficient by the flexural stress with the correct sign.

TABLE IV. - FORCE DEFORMATION RELATIONSHIPS FOR A $[45_{10}/-45_{10}]$ BORON EPOXY LAMINATE (27.9 cm (11.0 in) × 24.8 cm (9.75 in) × 0.28 cm (0.11 in) Ref. 13)

$$\begin{Bmatrix} \{N_c\} \\ \hdashline \{M_c\} \end{Bmatrix} = \begin{bmatrix} [A] & [C] \\ \hdashline [C] & [D] \end{bmatrix} \begin{Bmatrix} \{\epsilon_{co}\} \\ \hdashline \{X_c\} \end{Bmatrix}$$

$$\begin{bmatrix} [A] & [C] \\ \hdashline [C] & [D] \end{bmatrix} = \left[\begin{array}{ccc:ccc} 10.21 & 8.50 & 0 & 0 & 0 & -0.20 \\ 8.50 & 10.21 & 0 & 0 & 0 & -0.20 \\ 0 & 0 & 8.62 & -0.20 & -0.20 & 0 \\ \hdashline 0 & 0 & -0.20 & 1.01 & 0.84 & 0 \\ 0 & 0 & -0.20 & 0.84 & 1.01 & 0 \\ -0.20 & 0.20 & 0 & 0 & 0 & 0.85 \end{array}\right] \times (10^5 \text{ lb/in}^2)$$

or

$$\times (6.9 \times 10^2 \text{ MPa})$$

$$[D_R] = \begin{bmatrix} D_{11} & D_{12} & D_{13} \\ D_{21} & D_{22} & D_{23} \\ D_{31} & D_{32} & D_{33} \end{bmatrix} = \begin{bmatrix} 552 & 383 & 0 \\ 383 & 552 & 0 \\ 0 & 0 & 431 \end{bmatrix} \times (\text{lb/in})$$

or

$$\times (0.0069 \text{ MPa})$$

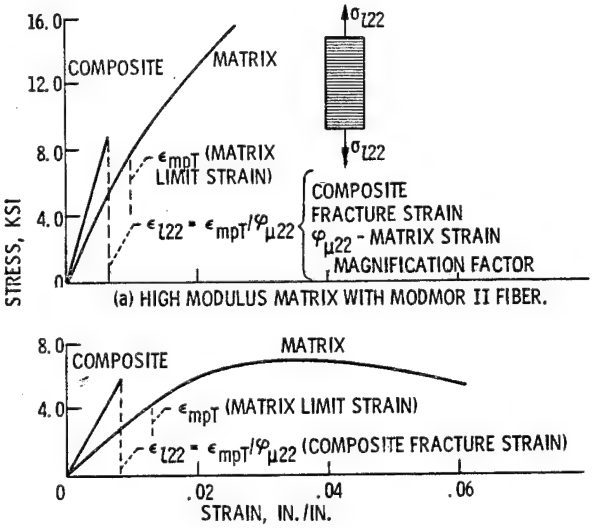

Figure 1. - Transverse composite and matrix stress/strain curves (ref. 1).

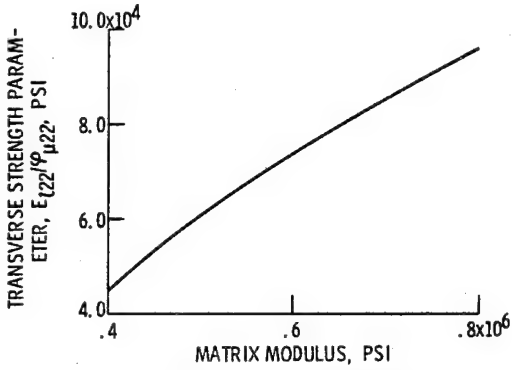

Figure 2. - Effect of matrix modulus on transverse strength parameter. TH-50/epoxy with 0.5 fiber volume ration and zero voids (ref. 1).

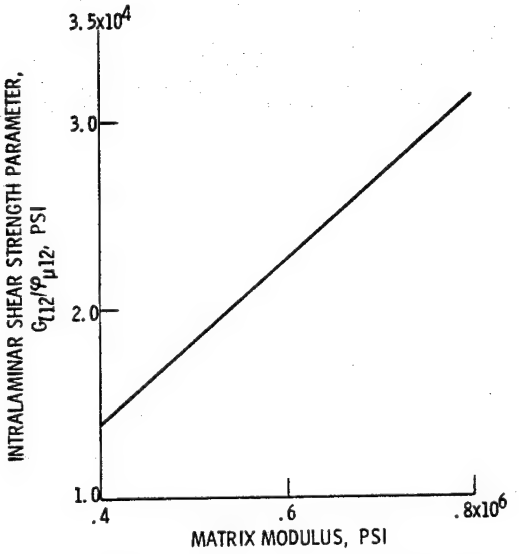

Figure 3. - Effect of matrix modulus on intralaminar shear strength parameter. TH-50/epoxy with 0.5 fiber volume ration and zero voids (ref. 1).

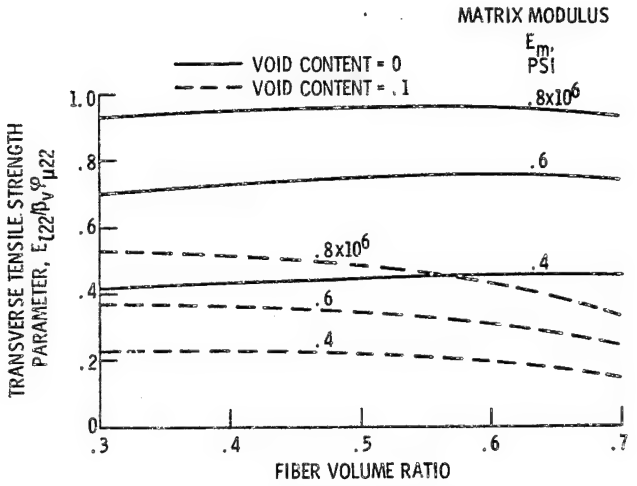

Figure 4. - Effects of Thornel-50/resin unidirectional composite transverse tensile strength limited by in situ matrix tensile strain (elongation) (ref. 1).

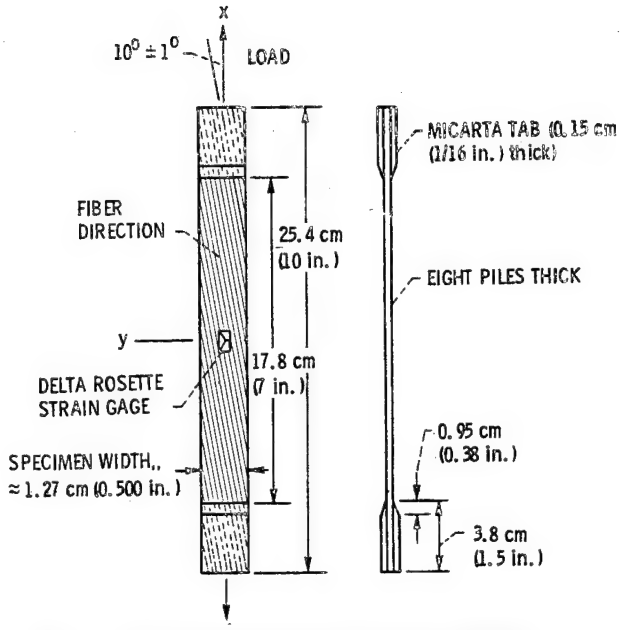

Figure 5. - Schematic showing geometry and instrumentation of proposed 10^o off-axis tensile specimen for fiber composite intralaminar shear characterization (ref. 3).

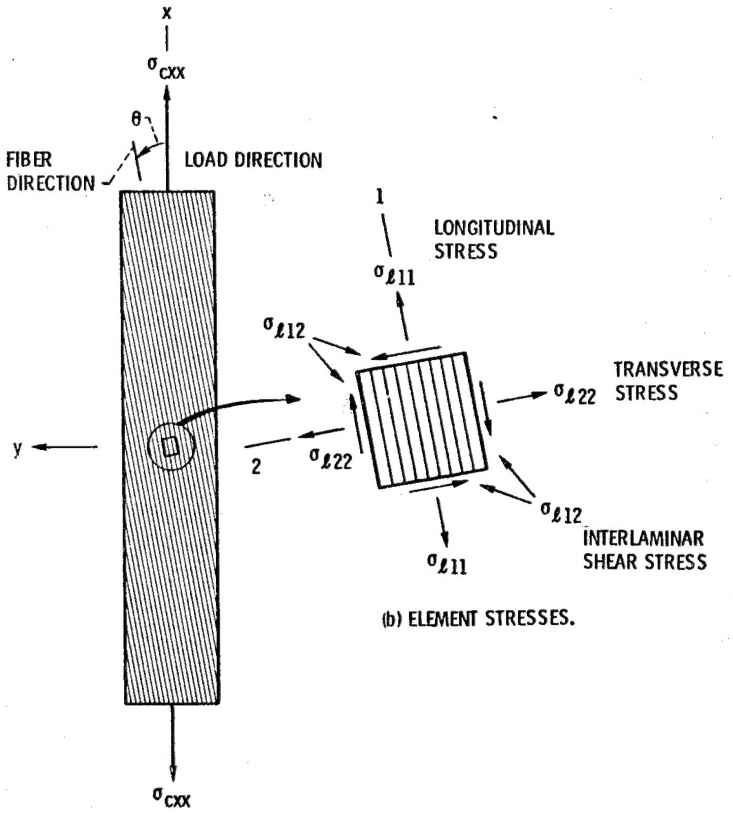

(a) LOADED SPECIMEN.

(b) ELEMENT STRESSES.

Figure 6. - Schematic depicting loaded 10^0 off-axis tensile test specimen and stresses at element at 10^0-plane (x, y - structural axes; 1, 2 - material axes) (ref. 3).

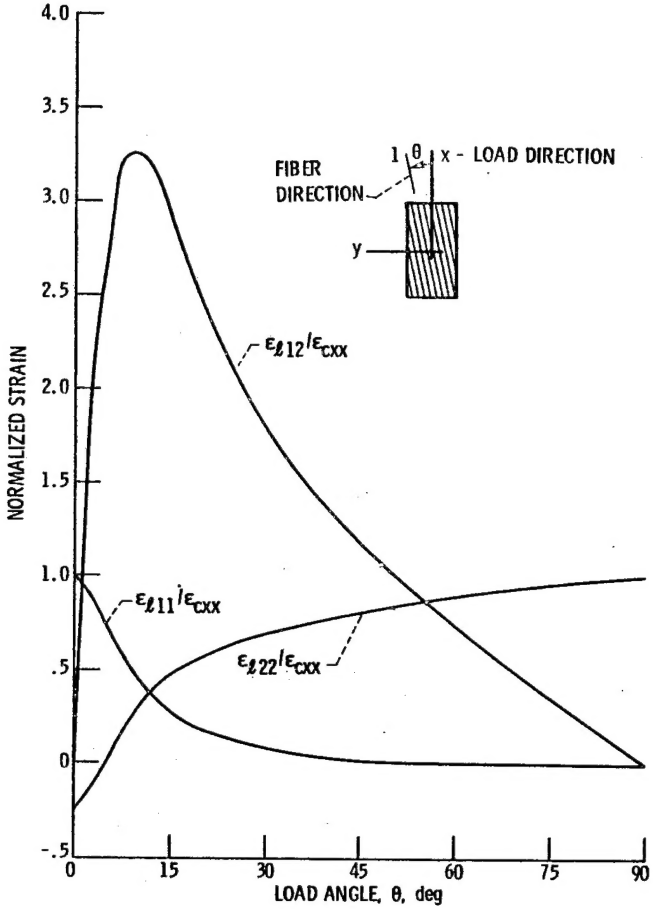

Figure 7. - Variation of material axes strains in unidirectional composite (Mod-I/epoxy) plotted against load direction (ref. 3).

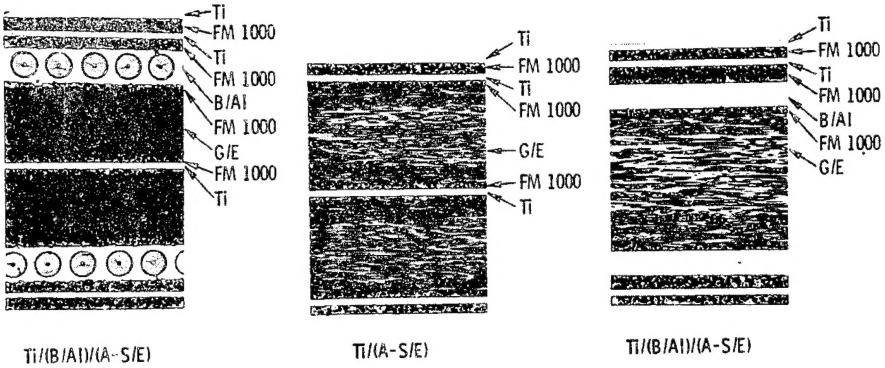

Figure 8. - Superhybrids. Composite specimen cross sections; (ref. 5).

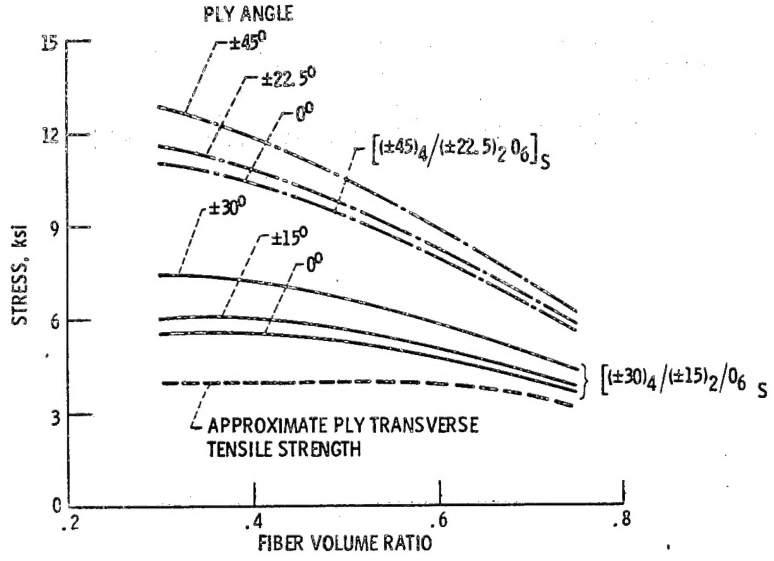

Figure 9. - Ply residual transverse stress for Modmor-I/polyimide composites. Temperature difference = -600° F (ref. 6).

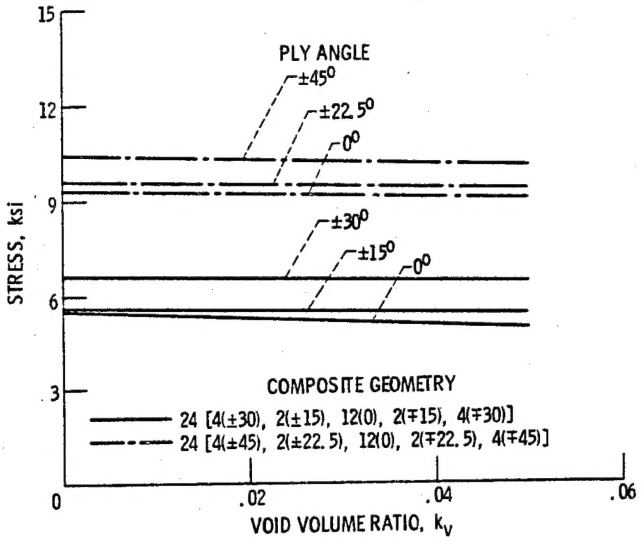

Figure 10. - Effects of voids on ply transverse residual stress. Modmor-I/polyimide composites. Fiber volume ratio = 0.50. Temperature difference = -600° F (ref. 6).

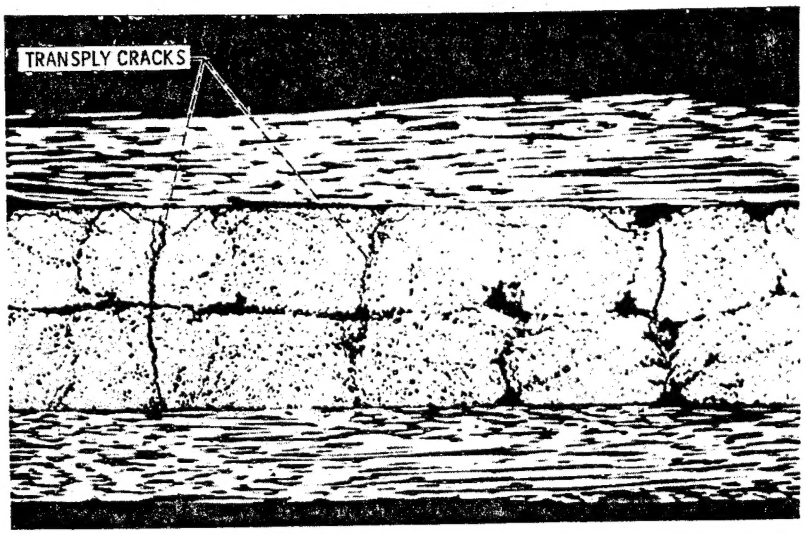

Figure 11. - Photomicrograph showing transply cracks $(0/90)_S$ high-modulus/epoxy.

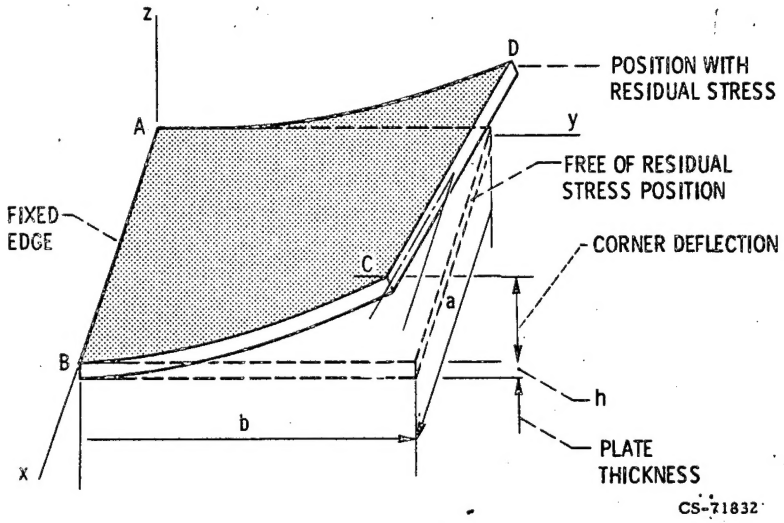

Figure 12. - Schematic depicting corner deflection due to warpage (ref. 10).

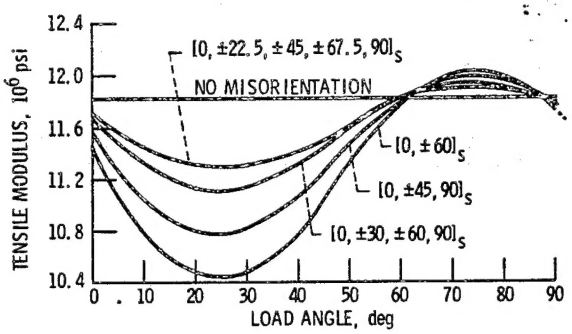

Figure 13. - Effect of 5^0 misorientation of 0^0 plies on the tensile modulus of quasi-isotropic laminates (ref. 12).

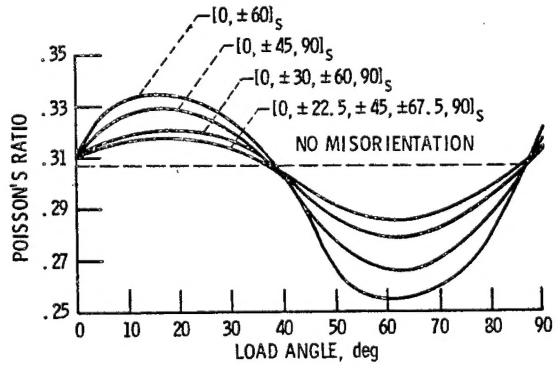

Figure 14. - Effect of 5^0 misorientation of 0^0 plies on the Poisson's ratio of quasi-isotropic laminates (ref. 12).